Facile preparation of antifouling nanofiltration membrane by grafting zwitterions for reuse of shale gas wastewater

Facile preparation of antifouling nanofiltration membrane by grafting zwitterions for reuse of shale gas wastewater

Minli Hu [a,b], *Qidong Wu* [a,b], *Chen Chen* [c], *Songmiao Liang* [d], *Yuanhui Liu* [a,b], *Yuhua Bai* [e], *Alberto Tiraferri* [f], *Baicang Liu* [a,b,*]

[a] Key Laboratory of Deep Earth Science and Engineering (Ministry of Education), College of Architecture and Environment, Institute of New Energy and Low-Carbon Technology, Institute for Disaster Management and Reconstruction, Sichuan University, Chengdu, Sichuan 610207, PR China

[b] Yibin Institute of Industrial Technology, Sichuan University Yibin Park, Section 2, Lingang Ave, Cuiping District, Yibin, Sichuan 644000, PR China

[c] Litree Purifying Technology Co., Ltd, Haikou, Hainan 571126, PR China

[d] Vontron Technology Co., Ltd, Guiyang 550018, PR China

[e] Infrastructure Construction Department, Chengdu University, Chengdu 610106, PR China

[f] Department of Environment, Land and Infrastructure Engineering, Politecnico di Torino, Corso Duca degli Abruzzi 24, 10129 Turin, Italy

Abstract: Complex organic matter causes severe fouling when membranes are applied for shale gas wastewater (SGW) treatment. This study reports the grafting of a zwitterionic polymer brush consisting of poly (sulfobetaine methacrylate) (PSBMA) onto the surface of a commercial nanofiltration (NF) membrane via electron transfer-atom transfer radical polymerization (ARGET-ATRP) to achieve anti-fouling property, especially against organic foulants. Compared to the pristine NF membranes, the PSBMA-grafted NF membrane showed high performance when challenged by SGW as a feed stream: (1) The productivity was significantly improved during long-term operation, with a 64.28% increase in flux at 50% recovery rate of SGW, while maintaining a near constant ion removal rate; (2) According to fluorescence regional integration under the Excitation—Emission—Matrix Spectra, the removal of protein-like organic matters and humus-like organic matters increased by 34.01% and 16.48%, respectively; (3) The XDLVO theory demonstrated that the hydrophobic interactions between the membrane surface and organic foulants were reduced by increasing the Lewis acid-base interaction energy. The proposed anti-fouling zwitterionic membranes has potential in industrial application for the on-site reuse of SGW.

Keywords: Shale gas wastewater (SGW); Membrane fouling; Surface modification; Poly (sulfobetaine methacrylate) (PSBMA); Nanofiltration (NF)

1. Introduction

The “shale gas revolution” was first successfully practiced in the USA to ensure energy security. China is currently accelerating the pace of shale gas exploration and development [1, 2]. According to evaluations made by the Chinese government, China has 25.08×10^{12} m^3 of technically recoverable shale gas reserves, positioning it as one of the most promising countries in the world for shale gas development [3, 4]. However, the shale gas exploration process consumes large amounts of freshwater resources and generates vast quantities of shale gas wastewater (SGW) [5, 6]. In the Sichuan Basin, China, the average freshwater demand of a shale gas well is 23,650–34,000 m^3, and 8-70% of the shale gas flowback and produced water is returned to the ground [7-9].

SGW in the Sichuan Basin contains low to moderate salinity (total dissolved solids < 30 g/L), complex and heterogeneous organic compounds, and its treatment to safe standard is costly and challenging [10]. Currently, most SGW both in China and USA are reused for fracturing in new wells, since the recycling of the fracturing fluid can achieve both cost savings and environmental pollution reduction [11-13]. The effective removal of divalent ions is critical for SGW reuse to avoid scaling on production equipment and in the shale formation [14-16]. Based on the salinity and composition of the Sichuan Basin SGW, nanofiltration (NF) membrane technology is a suitable and promising candidate for purification with the aim to remove divalent ions and maintain a stable production of shale gas [9, 17, 18]. However, membrane fouling is a major drawback that restricts the application of NF membranes and can lead to increased energy consumption, alongside increased frequency of chemical cleaning and shortened membrane life [19-21]. In general, membrane fouling is the result of a complex series of physicochemical interactions between the membrane surface and the fouling agents [21, 22][23, 24]. The complex organic mixture in SGW is arguably the main cause of NF membrane fouling in this application [25]. Effective pretreatments are often used

to improve the NF performance and ensure its sustainable operation [13, 26]. The combination of coagulation [27], adsorption [28], ozone pre-oxidation [29], or biological treatment technology [30] with UF has been applied for pre-treatment. However, NF fouling is still inevitable and few studies have focused on the properties of the NF membrane itself to improve their resistance to contamination from SGW foulants.

The synthesis of new antifouling membranes through surface modification is an effective way to control membrane fouling [22], and direct modification of the membrane surface is ideal for large-scale processing applications [31-33]. Antifouling membrane modification materials are mainly polymers, and the introduction of hydrophilic monomers or polar groups can significantly improve the membrane antifouling performance [34, 35]. Commonly used modifiers include: poly(vinyl alcohol) (PVA) [36], polyethylene glycol (PEG) [37], MXene [38], polydopamine (PDA) [39], and polyurethane[40]. Compared to other hydrophilic materials, zwitterionic polymer brushes (e.g., sulfobetaine methacrylate, SBMA) comprising both anionic and cationic end groups exhibit excellent antifouling performance at high salt concentrations [41], because of their overall electrical neutrality and strong hydration ability. SBMA can form a tight hydration layer on the surface of membrane materials, which can weaken the interaction force between organic pollutants and the membrane surface [21, 31, 41-48]. In particular, this mechanism is effective against hydrophobic organic substances, such as protein-like and humic-like matter, which accounts for a relatively high proportion of the organics in SGW [28, 29, 35, 49]. Typical modification methods include chemical grafting, physical coating, and polymer modification [44, 45, 47]. Modification through activators regenerated by electron transfer–atom transfer radical polymerization (ARGET-ATRP) is suitable to modify the membrane surface at large scale under routine industrial conditions in an easy and quick way, because it only require a low dosage of copper catalyst and has high tolerance to oxygen presence [50, 51]. Our previous study used ARGET-ATRP

method to graft [2-(methacryloyloxy) ethyl] dimethyl(3-sulfopropyl) ammonium hydroxide (DMAPS) on the surface of self-made green ultrafiltration membranes showing highly promising results also for other membrane processes and applications [52].

In this work, we tune and apply this procedure to fabricate a high-performance NF membrane deployed to treat SGW with the goal of reuse. The relationship between membrane surface modification and improved antifouling performance is investigated upon grafting a zwitterionic polymer brush PSBMA onto the surface of a commercial NF membranes via an ARGET-ATRP method. The water flux decline rate is analyzed and evaluated in the light of the membrane surface properties and the degree of organic deposition. The effect of membrane fouling is discussed using the XDLVO theory. The purpose of this paper is to provide valuable information on ways to reduce NF membrane fouling by designing NF membranes suitable for shale gas wastewater treatment.

2. Materials and methods

2.1. Pretreatment of the raw water

The raw water in this study was acquired from one of the reservoirs of the Weiyuan shale gas play, Sichuan, China. The detailed water quality and the optimal pretreatment conditions were comprehensively analyzed in our previous study [13]. In brief, the optimal pretreatment condition for coagulation involved addition of 900 mg/L ferric chloride hexahydrate ($FeCl_3 \cdot 6H_2O$) followed by 30 min settling. The supernatant was then introduced to the tank of a ultrafiltration system comprising a submerged hollow fiber poly (vinylidene fluoride) (PVDF) UF membrane (Litree Purifying Technology Co., Ltd. Haikou, China with nominal molecular weight cut-off 100 kDa under a constant flux of 50 L $m^{-2}h^{-1}$).

2.2. Materials

Two types of commercially available NF membranes were employed in this work, namely, the membranes referred to as VNF1 (Vontron Membrane Technology Co., Ltd., Guiyang, China), and NF90 (DuPont, USA). Ultrapure water was supplied by a Ulupure ultrapure water purification system (Chengdu, China) with a resistivity of 18.25 MΩ. Sulfobetaine methacrylate (SBMA), sometimes referred to as 3-dimethyl (methacryloyloxyethyl) ammonium propane sulfonate (DMAPS), N,N-dimethylformamide (DMF)，l-ascorbic acid, copper (II) chloride, tris (2-pyridylmethyl) amine (TPMA), magnesium sulfate ($MgSO_4$, anhydrous, reagent plus, ⩾99.5%), and sodium chloride (NaCl, reagent grade, 99%) were obtained from Sigma Aldrich (USA), Dopamine hydrochloride, α-bromoisobutyryl bromide (BiBB, 98%), isopropyl alcohol (IPA), tris (hydroxymethyl) aminomethane (Tris) (>99.8%), and triethylamine (TEA) (>99%), were purchased from Aladdin (China). Sodium sulfate (Na_2SO_4) (anhydrous, ⩾99%), magnesium chloride ($MgCl_2$) (⩾98%), and ethylene glycol (99%) were all analytical reagents (Kelong Chemical, Chengdu, China). Glycerol (99.7%) was purchased from VWR (PA, USA). Diiodomethane (99%) was purchased from Macklin (Shanghai, China).

2.3 Surface modification of NF membranes

The commercial membrane was subject to surface ARGET-ATRP grafting reaction through a typical three-step strategy. The first step involved the preparation of a BiBB-initiator-dopamine solution; after addition of the Tris buffer into this solution to adjust the pH, the commercial membrane was placed into the buffered solution to form a PDA surface coating (seond step); the third step encompassed the grafting of SBMA to the membrane surface through the ARGET-ATRP reaction. The detailed steps can be found in **Text S1 (SI)**.

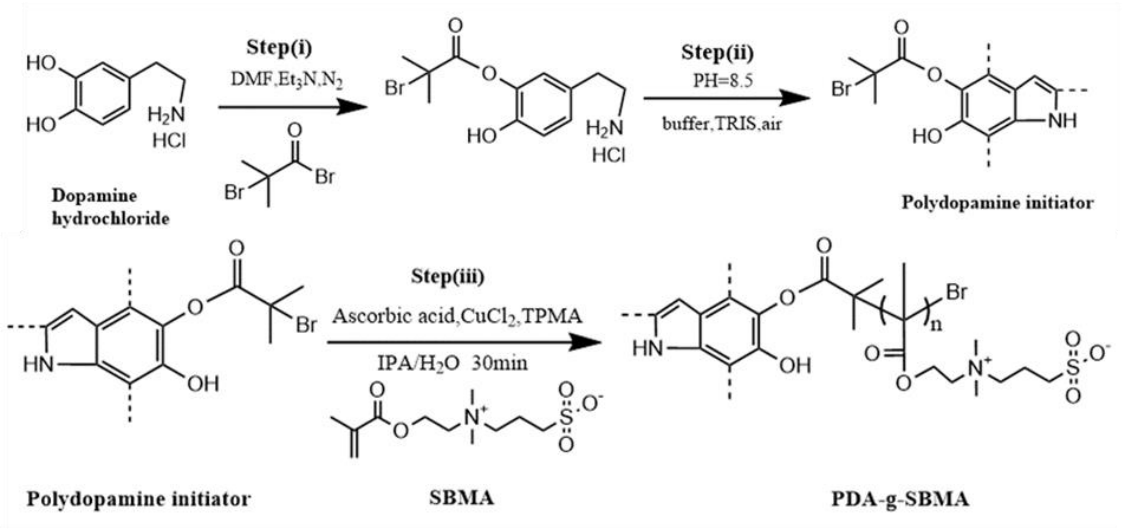

Scheme. 1. Proposed modification of NF membranes and reaction products: Step (i) involved the reaction of dopamine hydrochloride and 2-bromoisobutyryl bromide; Step (ii) in which the reaction mixture from Step (i) was added to Tris buffer (pH=8.5) to form a BiBB-initiator-PDA coating; Step (iii) involved the surface initiated ARGET-ATRP reaction with SBMA from the BiBB-initiator-PDA coating to produce modified membranes with a surface-grafted SBMA polymer brush.

2.4. Membrane Characterization

The surface chemical composition of the membranes was analyzed via X-ray photoelectron spectroscopy (XPS) (Axis Supra, Kratos Analytical Ltd., UK) and with a Fourier transform infrared (FTIR) spectrometer equipped with a diamond attenuated total reflection (ATR) attachment (Nicolet is iS20, Thermo Fisher Scientific Inc., USA). The membrane surface morphology and roughness characteristics were obtained by scanning electron microscopy (SEM) (Regulus 8230, Hitachi, Japan) and atomic force microscopy (AFM, Dimension Icon, Bruker, Germany), respectively. The zeta potential was evaluated by a SurPASS^{TM} 3 electrokinetic analyzer (Anton Paar, Austria). The dynamic water contact angles were determined by a contact angle measurement equipment (KRÜSS GmbH, Germany) at room temperature. More details can be found in our previous study [53] and in **Text S2 (SI)**.

2.5 Separation performance of the NF membranes

The NF lab unit was thoroughly cleaned before and after each fouling experiment. Prior to each experiment, the membranes were soaked in ultrapure water at room temperature for 24 h and then compacted with ultrapure water at a pressure of 6.89 bar (100 psi) for at least 30 min. The separation performance of the membranes was evaluated at an applied pressure of 20.7 bar (300 psi) in a stainless-steel dead-end membrane module (HP 4750, Sterlitech Corp., Kent, WA), with an effective testing area, A, of 14.6 cm^2. The separation equipment was operated under constant stirring of 300 rpm to minimize concentration polarization effects. Eq. (1) was employed to determine the flux of pure water:

$$J = \frac{V}{A \times \Delta t} \qquad (1)$$

where V (L) is calculated by dividing the permeate water mass collected in a certain interval (Δt) by the water density.

The ion filtration performance of the NF membranes was evaluated using inorganic salts (Na_2SO_4, $MgSO_4$, $MgCl_2$, NaCl) in water with a concentration of 2000 mg/L. The salt solute rejection (R) was obtained at steady-state by Eq (2).

$$R = 1 - \frac{C_p}{(C_0 + C_f)/2} \qquad (2)$$

where C_P and C_0 represent the concentration of the solute in the permeate and that in the feed, respectively, while C_f is the concentration of the solute in the final concentrated feed. Electric conductivity measured by calibrated ultrameter II 6PFC conductivity meter (Myron L Company) was used as a proxy for salt concentration. The presented rejection values for each sample are the average of three different measurements collected over a 60 min period.

2.6 Anti-fouling properties

The normalized permeate flux in the fouling stage was calculated using Eq. (3) [54][59]:

$$normalized\ \ flux = \frac{J}{J_0} \tag{3}$$

where J is the permeate flux at any given time during the test, and J_0 is the initial permeate flux. The slope of the plot of J/J_0 versus recovery rate (%, v/v) yielded the fouling propensity of the NF membranes [54].

To determine the surface tension characteristics of a solid surface, two of the three probe liquids should be polar and the other should be non-polar, and the test reagents must have high surface tension parameters [55]. In this study, the surface of the pristine NF membranes and the modified NF membranes are regarded as solid. The two polar liquids were ultrapure water and glycerol, while the non-polar liquid was diiodomethane. The surface tension properties of each probe liquid are listed in **Table S1 (SI)**. The surface tension parameters of the materials were calculated by measuring the direct contact angle of the three probe liquids and using a modified form of the extended Young equation given by:

$$\gamma_{L}^{TOT} = \gamma_{L}^{LW} + \gamma_{L}^{AB} \tag{4}$$

$$\gamma_{L}^{AB} = 2\sqrt{\gamma_{L}^{+}\gamma_{L}^{-}} \tag{5}$$

$$(1+\cos\theta)\gamma_{L} = 2\left(\sqrt{\gamma_{S}^{LW}\gamma_{L}^{LW}} + \sqrt{\gamma_{S}^{+}\gamma_{L}^{-}} + \sqrt{\gamma_{S}^{-}\gamma_{L}^{+}}\right) \tag{6}$$

According to the ‘extended DLVO’ or ‘XDLVO’ theory, in the water environment, the interfacial energy between membranes and foulants is the sum of the Lifshitz–van der Waals (LW), electrostatic double layer (EL), and Lewis acid–base (AB) interactions. The electrostatic force (EL) interaction energy (ΔG_{mlf}^{EL}) is also one component of the total interaction free energy, but it is much smaller than ΔG_{mlf}^{TOT} , and can thus be neglected, resulting in:

$$\Delta G_{mlf}^{TOT} = \Delta G_{mlf}^{LW} + \Delta G_{mlf}^{AB} \tag{7}$$

196 $$\Delta G_{mlf}^{LW} = -2(\sqrt{\gamma_f^{LW}} - \sqrt{\gamma_l^{LW}})(\sqrt{\gamma_m^{LW}} - \sqrt{\gamma_l^{LW}}) \quad (8)$$

197 $$\Delta G_{mlf}^{AB} = 2[\sqrt{\gamma_l^+}(\sqrt{\gamma_m^-} + \sqrt{\gamma_f^-} - \sqrt{\gamma_l^-}) + \sqrt{\gamma_l^-}(\sqrt{\gamma_m^+} + \sqrt{\gamma_f^+} - \sqrt{\gamma_l^+}) - (\sqrt{\gamma_m^+\gamma_f^-} + \sqrt{\gamma_m^-\gamma_f^+})] \quad (9)$$

198 The subscripts f, l, and m represent the foulant, the liquid medium, and the membrane
199 surface, respectively. Statistical analysis was performed with the statistical software SPSS
200 18.0.

201 **3. Results and discussion**

202 3.1 Membrane surface properties

203 Membrane surface characteristics, such as chemical structure, hydrophilicity, roughness,
204 and charge determine the separation performance and the anti-fouling properties of the
205 membrane [42, 56]. **Fig. 1(A)** presents that the ATR-FTIR spectra determined between 500
206 cm^{-1} and 4000 cm^{-1} for the pristine NF90 and VNF1 membranes, the BiBB-initiation-PDA
207 mobilized membranes (NF90-PDA, VNF1-PDA), and the PDA-g-PSBMA modified NF
208 membranes (NF90-PSBMA, VNF1-PSBMA). The stretching vibration peak at 1578, 1504,
209 1487 cm^{-1} is attributed to the superposition of the peak of the polyamide layer and the
210 polysulfone layer in the benzene ring plane. The characteristic peaks of the polysulfone
211 support layer can be observed: specifically, the symmetric stretching vibration peaks of
212 O=S=O at 1167 and 1149 cm^{-1}, and the asymmetric stretching vibration peaks of O=S=O at
213 1320 and 1296 cm^{-1}. VNF1 series membranes are significantly different from NF90 series
214 membranes in that only the latter showed peaks at 1610 cm^{-1} (H-bonded C=O stretching) and
215 1540 cm^{-1} (N–H in-plane bending and C–N bending vibration stretching vibration of the
216 group –CO–NH-, amide II band) [57, 58]. Therefore, the characteristic peaks of amide II and
217 arylamide were not observed for the VNF1 series membranes, suggesting that the latter
218 consist of piperazine amide. The common peak between the two membranes at 1664 cm^{-1} is
219 attributed to the amide I band (C=O and C-N stretching vibration, C-C-N deformation
220 vibration) [59, 60]. After the grafting of the PSBMA brushes, new peaks at 1715 and 1038

cm^{-1} emerged, attributed to ester and sulfonate groups of SBMA, respectively. These results preliminarily indicate that PSBMA was successfully grafted on the NF membrane surfaces [48, 61].

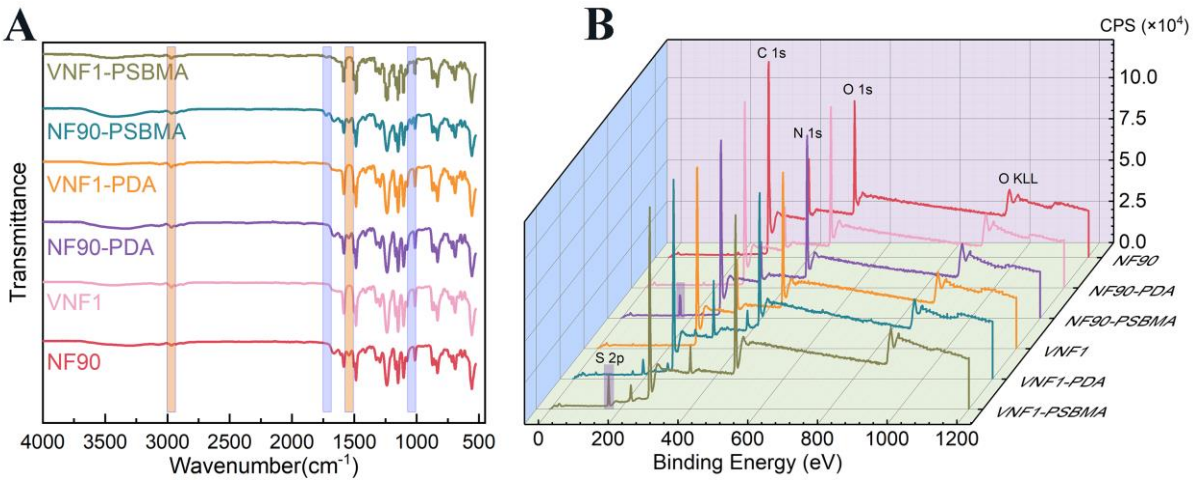

Fig. 1. (A) ATR-FTIR spectra and **(B)** XPS spectra of pristine NF90 and VNF1 membranes and modified membranes prepared from PDA immobilization and PSBMA grafting.

To further analyze the chemical composition of the NF90/VNF1 membrane surfaces before and after modification, XPS analysis was conducted and the resulting surface elemental compositions and spectra are presented in **Table 1** and **Fig. 1(B)**, respectively. An obvious increase in the O atom content and a decrease in N atom content were clearly observed upon PBSMA grafting. Consequently, the O/C atomic ratios of NF90-PSBMA and VNF1-PSBMA were respectively higher than those of NF90 and VNF1, while the N/C atomic ratios were lower. This result is rationalized with the fact that the grafted PSBMA has high O/C atomic ratio and low O/N atomic ratio compared with the pure polyamide. These results further confirm that PSBMA was successfully introduced onto the NF membrane surfaces.

Table 1 Surface elemental composition of the membranes.

Membrane No.	Atomic percent (%)	Atomic ratio

	C	N	O	Br	O/N	O/C
NF90	74.29	10.56	15.15	0	1.43	0.20
NF90-PDA	72.86	7.63	19.47	0.04	2.55	0.27
NF90-PSBMA	72.33	7.33	20.31	0.03	2.77	0.28
VNF1	74.52	8.54	16.81	0	1.97	0.23
VNF1-PDA	75.04	8.14	16.76	0.13	2.06	0.22
VNF1-PDA	73.64	4.62	21.67	0.07	4.69	0.29

239

240 3.2. Morphology analysis and surface charge

241 The morphology and roughness of the membrane surface influence the membrane
242 hydrophilicity, water flux, and the interactions between the surface and foulants. The surface
243 morphology of the NF90 and VNF1 membranes did not change significantly upon
244 modification with PSBMA (**Fig. 2**). According to the AFM results, the root means square
245 roughness parameters (Rq) of the NF90, NF90-PDA, and NF90-PSBMA membrane were
246 54.4±2.1 nm, 38.7±3.7 nm, and 29.0±0.6 nm, respectively, while those of VNF1, VNF1-PDA,
247 and VNF1-PSBMA membrane were 5.04±0.1 nm, 4.68±0.2 nm, and 3.87±0.7 nm,
248 respectively. Therefore, the roughness of the membrane surfaces decreased by approximately
249 20% after coating with PDA and by approximately 45% upon modification with the
250 zwitterion, with respect to the pristine membranes (**Fig. 3A**). This result suggest that the
251 modification steps may level out the surface features of polyamide. However, the initial
252 roughness of the two membranes was already small and the observed reduction was not
253 substantial in absolute terms, thus likely not resulting in significant changes in membrane
254 performance during operation.

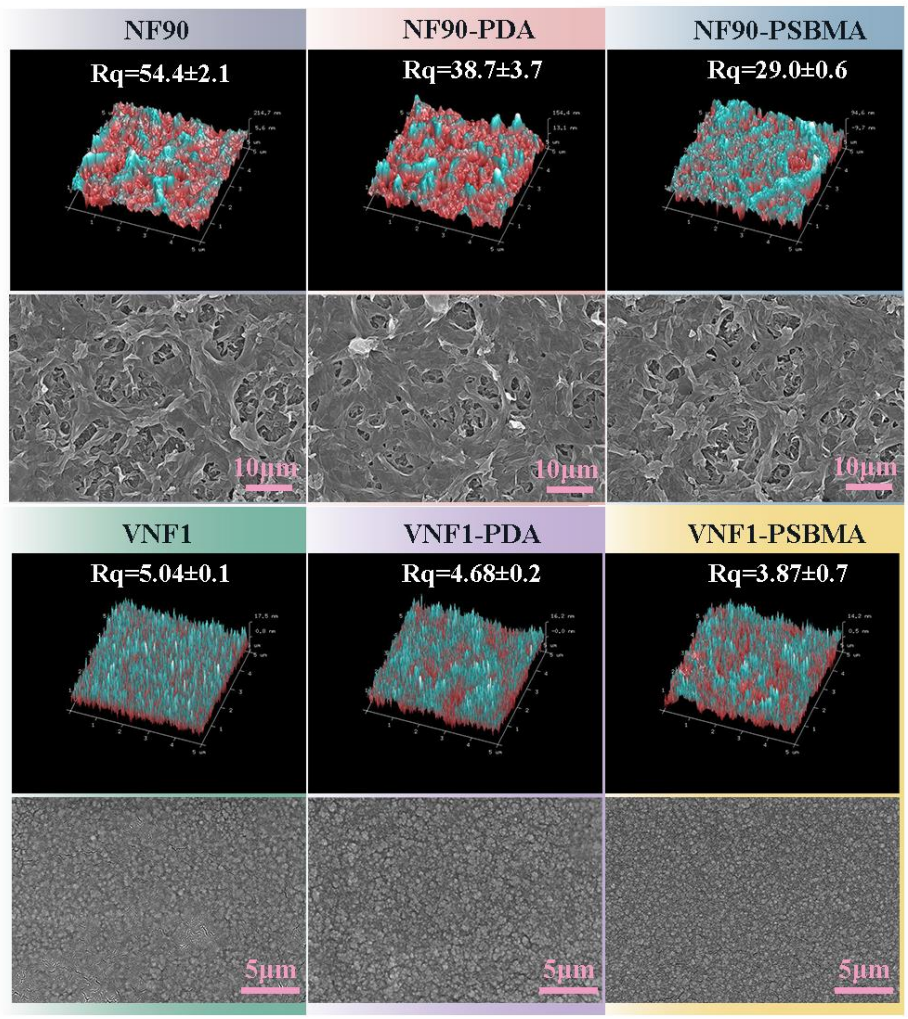

255

256 **Fig. 2.** AFM and SEM images of pristine NF90 and VNF1 membranes and modified

257 membranes prepared by immobilizing PDA and by grafting PSBMA.

258

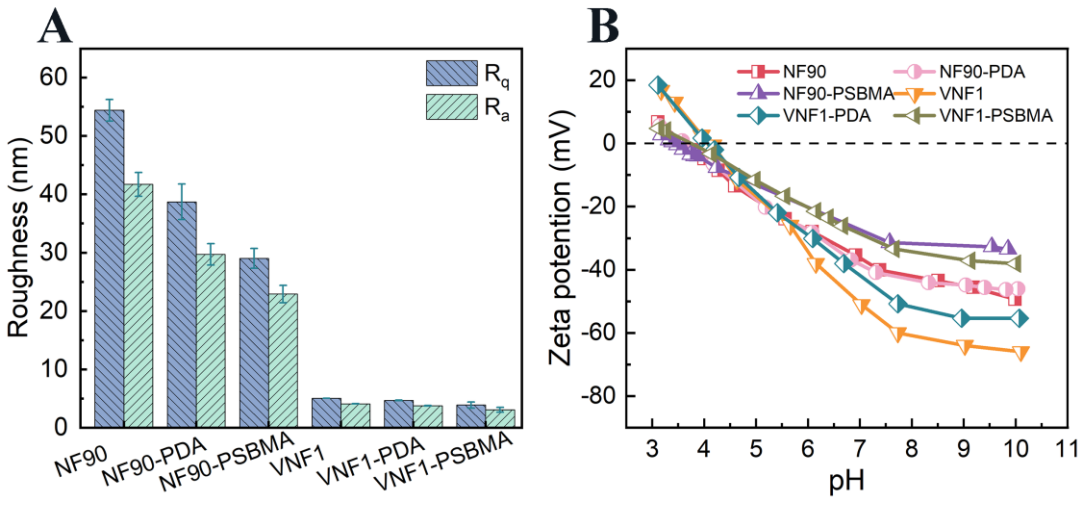

259

Fig. 3. (A) The average values of root mean-square (Rq) and average roughness (Ra) were calculated from AFM images using at least six different locations on each membrane sample (NF90, NF90-PDA, NF90-PSBMA, VNF1, VNF1-PDA and VNF1-PSBMA); **(B)** Surface zeta potential values of pristine NF90 and VNF1 membrane and modified membranes as a function of pH.

The surface properties of the modified membranes were further investigated by acquiring zeta potential values. As shown in **Fig. 3B**, the pristine NF90 and VNF1 membranes had highly negative electric potential, due to the carboxyl groups typically resulting from interfacial polymerization of polyamide. With the coating of PDA, the amine and hydroxyl groups of dopamine generally reduced the magnitude of the negative potential, which was then further reduced upon SBMA grafting due to the net zero charge properties of the zwitterions [62]. This trend was more pronounced in the VNF1 membrane samples, for which a potential of larger magnitude was measured at the surface of the pristine membrane. However, the zeta potential curves of the membranes modified with the PSBMA brush layer was practically thre same, regardless of the starting material, suggesting that the modification was successful in both cases.

The wettability of the membrane surface was evaluated through water contact angle measurements **(Fig. 4A**). The initial contact angles of pristine NF90 membrane, NF90-PDA membrane, and NF90-PSBMA membrane were 55.2±0.9°, 48.7±1.5°, and 46.0±2.3°, respectively, while the initial contact angles of pristine VNF1 membrane, VNF1-PDA membrane, and VNF1-PSBMA membrane were 52.5±1.9°, 41.6±2.65°, and 28.4±0.99°, respectively. The presence of PDA increased the wettability, although this enhancement effect was minor, owing to the short reaction time (10 min). On the other hand, the water contact

angle decreased significantly after growth of the zwitterionic polymers brush, especially for the VNF1 samples.

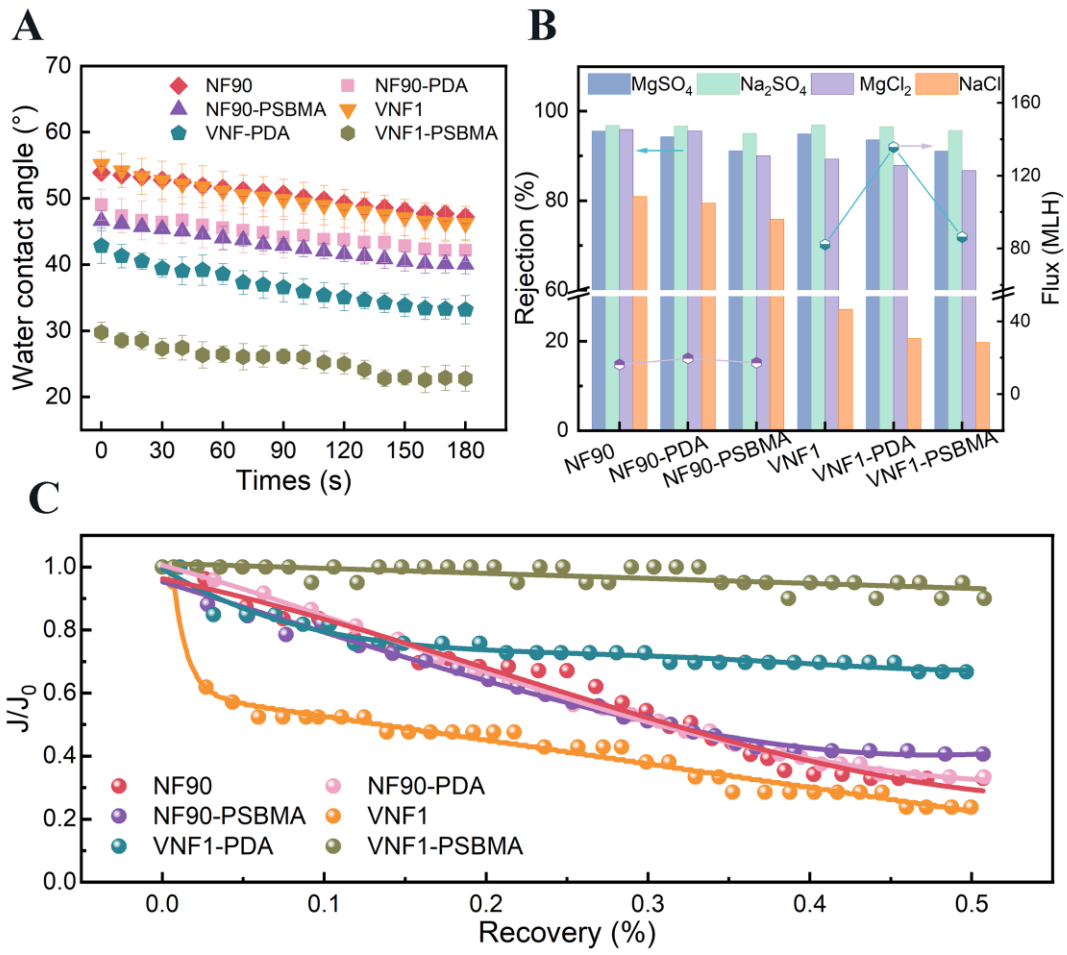

Fig. 4. (A) Water contact angle variation in time of pristine NF90 and VNF1 membranes and modified membranes; **(B)** Salt rejection values of pristine NF90 and VNF1 membrane and modified membranes (2.068 MPa, 25 °C, salt concentration: 2000 mg/L); **(C)** Permeate flux as a function of tecovery rate for the different membranes (operating pressure: 2.068MPa; maximum water recovery: 50%).

Considering the selectivity shown in **Fig. 4B**, all the membranes had much higher rejection to divalent ions than monovalent ions, exhibiting a typical NF performance. In general, the observed rejection was in the order Na_2SO_4 > $MgSO_4$ > $MgCl_2$ > NaCl. With the coating of dopamine and the grafting of PSBMA, the retention rate of all the ions was slightly reduced,

but overall, there was no significant loss of the original retention rate. During filtration of ultrapure water, the average flux were 16.2, 19.7, and 17.3 LMH for NF90, NF90-PDA and NF90-PSBMA, while the permeate flux of VNF1-based samples were much higher, with average fluxes equal to 82.2, 135.6, and 86.3 LMH for VNF1, VNF1-PDA and VNF1-PSBMA, respectively. Compared to the VNF1 membranes, the NF90 membranes are denser and therefore provide higher retention of monovalent ions and correspondingly lower fluxes. In both cases, the flux increased significantly following PDA coating and returned to lower values upon zwitterion brush formation. Ultimately, the values observed for the zwitterion-grafted membranes were slightly higher than those measured for pristine membranes.

Fig. 4C illustrates the fouling behavior (revealing itself as a decrease in permeate flux [63]) of the membranes during the dead-end NF process for feed streams coinciding with the effluents of integrated coagulation-UF pre-treatment. Grafting of SBMA greatly improved the resistance to foulant deposition and to flux reduction. While the water flux was reduced compared to the membranes with only PDA attached, the performance of the membranes modified with PSBMA brushes was maintained for a longer period of time. The effect of VNF1 modification was significantly better than that of NF90, consistent with the results of FTIR and previous literature reports [13], likely due to the different chemistry of the polyamide constituting the two membranes. The flux measured by deploying the VNF1-PSBMA membrane was nearly constant during the filtration test, indicating negligible or inconsequential deposition of foulants on these samples.

It is usually difficult to draw an overall profile of organic pollutants in shale gas wastewaters and their process variations. Three-dimensional excitation-emission matrix (EEM) fluorescence spectroscopy was used to analyze fluorescent organics compositions in a complicated system such as the SWG of this study, by simultaneously varying the excitation and emission wavelengths in real time (**Fig. 5**) [64]. As detailed in our previous study [29],

the fluorescence regional integration (FRI) method allowed classification of the organic compounds in five domains: region I (Ex/Em = 220–250/280–330 nm, aromatic protein), region II (Ex/Em = 220–250/330–380 nm, aromatic protein), region III (Ex/Em = 220–250/380–480 nm, fulvic acid-like matters), region IV (Ex/Em = 250–440/280–380 nm, soluble microbial by-product-like matters), and region V (Ex/Em = 250–400/380–540 nm, humic acid-like components). According to the FRI under the EEM corresponding to each region volume, almost no removal of dissolved organic matter was achieved after coagulation, while the hybrid UF process mainly remove fulvic acid-like components, humic acid-like components, and phenolic compounds (**Fig 6B**). The fraction of dissolved organics removed by NF90 membrane was 94.1% for region III, 93.5% for region V, 87.7% for region II, 74.6% for region IV, and 37.9% for region I. Larger removal rates were observed for the modified NF90-PSBMA membranes, but in the same order: III (96.3%), V (95.4%), II (91.2%), IV (88.7%), I (83.7%). The same order of removal rate was also determined for VNF1 samples, with a higher rate relative to the modified membrane with respect to the pristine one. Specifically, while the removal rate of dissolved organics by VNF1 was III (85.8%), V (84.2%), II (78.6%), IV (51.1%), I (8.2%), that provided by VNF1-PSBMA was III (93.7%), V (91.7%), II (90.5%), IV (85.5%), I (80.3%). These results and those presented in **Fig. 5** clearly shows that the modified membranes improved the removal rate of organic matter in each of the areas, but more markedly that of protein-like organic matter, which may be due to the combination of increased membrane density and hydrophilicity following the surface modification.

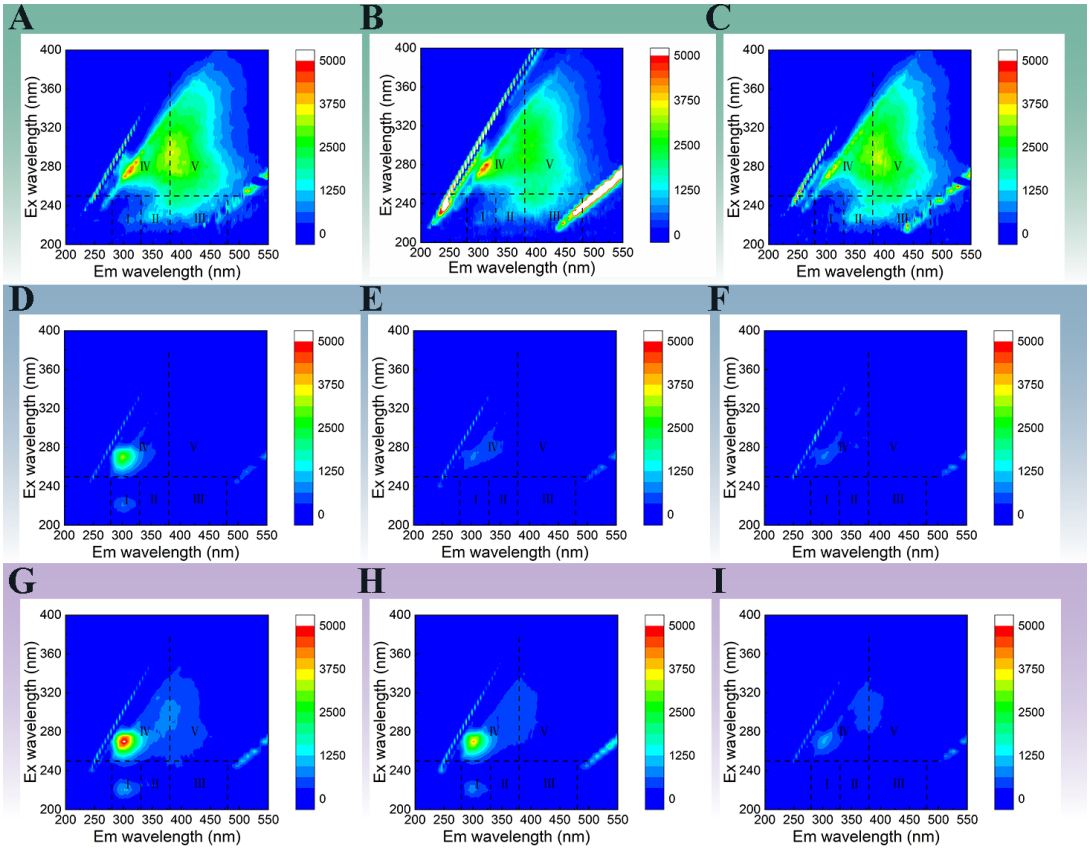

Fig. 5. Fluorescence excitation-emission matrix (EEM) of effluent water from each treatment process: (A) Raw water; (B) Coagulation; (C) Ultrafiltration; filtration through (D) NF90, (E) NF90-PDA, (F) NF90-PSBMA (G) VNF1, (H) VNF1-PDA, or (I) VNF1-PSBMA membranes. (I: tyrosine protein-like substances, II: tryptophan protein-like substances, III: fulvic-like substances, IV: soluble microbial byproducts, V: humic-like substances.)

3.4. Membrane-foulant physicochemical interactions

Extended XDLVO calculations are an accepted method to account for the interfacial forces between two surfaces at the microscopic scale [65]. In this paper, this theory was applied to investigate the main forces acting between the NF membranes and the SGW colloids. The contact angles of water, glycerol, and diiodomethane on the membrane surface and when in contact with a layer of SGW colloids are summarized in **Table S2 (SI)**. The resulting surface energy components (γ^{LW}, γ^{+}, γ^{-}) were calculated using **eqs. 4-6**, and the

results are shown in **Table 2**. ΔG_{mlf}^{LW} and ΔG_{mlf}^{AB} were thus obtained with **eqs. 8** and **9**, respectively, and the results are also presented in **Table 2**. Following surface grafting of the zwitterionic polymers SBMA, the electron acceptor component (γ^+) slightly increased, while the electron donor component (γ^-) increased importantly. This phenomenon is rationalized mainly with the fact that the -SO_3 group of SBMA is negatively charged in water, and can enhance the electron donating capability, hence the hydrophilicity of the membrane surface [52]. Repulsion forces thwart the adsorption of contaminants on the membrane surface: the more positive is the interaction energy, the more it is repulsive, and the membrane surface is less likely to be fouled [66, 67]. Both AB and LW components of the membranes-SGW colloids interaction had positive sign, thus the total interaction free energy (ΔG_{mlf}^{TOT}) had positive sign for all the membrane samples. Significantly, the surface grafting of SBMA provided much more positive values of the total interfacial free energy, implying that the zwitterionic SBMA brushes effectively reduced the likelihood of foulant adhesion on the membrane surfaces. Furthermore, we found that the Lewis acid-base interaction energy (ΔG_{mlf}^{AB}) was much higher than the Lifshitzvan der Waals interaction energy (ΔG_{mlf}^{LW}) and that ΔG_{mlf}^{LW} remained almost unchanged after surface grafting, while ΔG_{mlf}^{AB} increased significantly. Therefore, the Lewis acid-base interaction energy (ΔG_{mlf}^{AB}) played the key role in controlling membrane fouling.

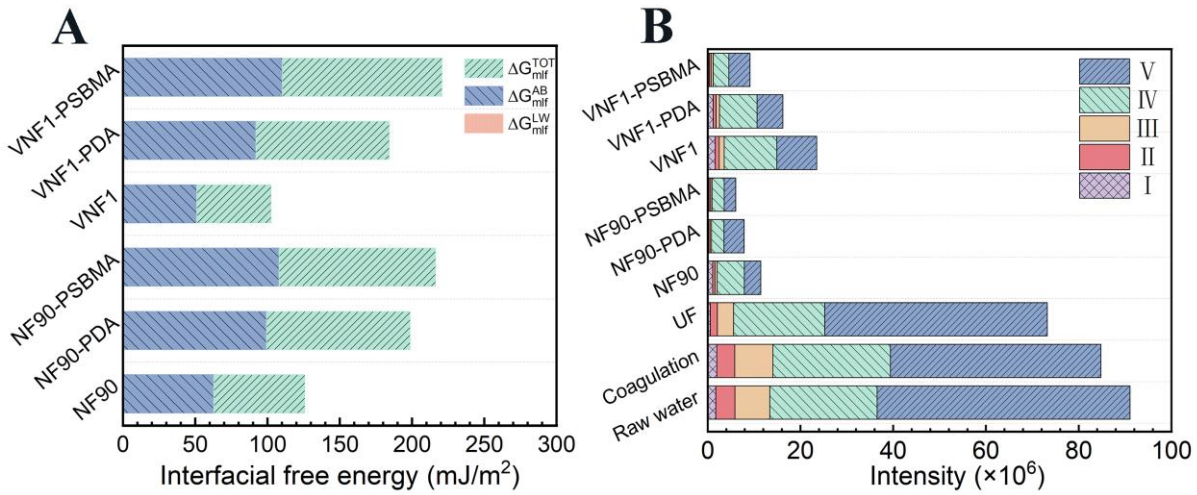

375

376 **Fig. 6. (A)** Total interaction energy (ΔG_{mlf}^{TOT}), Lifshitz–van der Waals interaction energy

377 (ΔG_{mlf}^{LW}), and Lewis acid–base (AB) interaction energy (ΔG_{mlf}^{AB}) between the membranes and

378 the SGW particles in aqueous solution; **(B)** Fluorescence region integral (FRI) results for

379 samples from the effluent of each treatment process.

380

381 **Table 2**

382 The surface tension parameters and interfacial free energy of all membranes and SGW

383 particles (mJ/m^2).

Item	Surface tension parameter (mJ/m^2)					Free Energy		
	γ_L^{LW}	γ_L^-	γ_L^+	γ_L^{AB}	γ_L^{TOT}	ΔG^{LW}	ΔG^{AB}	ΔG^{TOT}
NF90	33.956	21.135	0.156	3.626	37.582	0.516	62.341	62.857
NF90-PDA	33.388	42.664	0.004	0.797	34.185	0.494	98.839	99.333
NF90-PSBMA	30.249	49.483	0.002	0.568	30.818	0.370	107.746	108.116
VNF1	33.608	20.041	2.224	13.354	46.961	0.502	50.695	51.198
VNF1-PDA	33.759	37.450	0.005	0.899	34.659	0.508	91.573	92.081
VNF1-	30.456	53.440	0.113	4.921	35.377	0.378	109.957	110.336

PSBMA

Conclusion

Zwitterionic SBMA brushes were grafted onto the surface of commercial NF membranes, greatly improving the membrane antifouling ability and organic removal while retaining high values of water permeability and only slightly decreasing the rejection rate of conventional monovalent and divalent ions. The VNF1-PSBMA membrane exhibited very high performance with pure water flux of 86.3 LMH, sodium sulfate removal rate of 95.67%, and with the J/J_0 ratio upon fouling 73.54% higher than that related to the pristine VNF1 membrane at 50% recovery of SGW. All the dissolved organics were removed effectively by the VNF1-PSBMA membrane, but especially the protein-like organic matter, which was not rejected effectively by the pristine membranes. Antifouling and organic removal experiments showed that the modification of membranes with grafted zwitterionic has high potential to control membrane fouling and improve membrane performance in SGW reuse. This work proposes a membrane modification that effectively affords better membrane performance, particularly for the treatment of a highly complex wastewater from the shale gas industry, thus providing a successful exploration of modified membrane materials and industrial applications.

Acknowledgments

This work was supported by the National Natural Science Foundation of China (52070134, 51678377), Xinglin Environment Project (2020CDYB-H02), and Sichuan University and Yibin City People's Government strategic cooperation project (2019CDYB-25). We would like to thank the Institute of New Energy and Low-Carbon Technology,

Sichuan University, for SEM measurement and the Analytical & Testing Center of Sichuan University for XPS work and we would be grateful to Suilin Liu for his help of XPS analysis.

References

[1] C. Jia, M. Zheng, Y. Zhang, Unconventional hydrocarbon resources in China and the prospect of exploration and development, Petroleum Exploration and Development, 39 (2012) 139-146.

[2] H. Chang, T. Li, B. Liu, R.D. Vidic, M. Elimelech, J.C. Crittenden, Potential and implemented membrane-based technologies for the treatment and reuse of flowback and produced water from shale gas and oil plays: A review, Desalination, 455 (2019) 34-57.

[3] C.L. Weber, C. Clavin, Life Cycle Carbon Footprint of Shale Gas: Review of Evidence and Implications, Environ. Sci. Technol., 46 (2012) 5688-5695.

[4] S. Jiang, J. Zhang, Z. Jiang, Z. Xu, D. Cai, L. Chen, Y. Wu, D. Zhou, Z. Jiang, X. Zhao, S. Bao, Geology, resource potentials, and properties of emerging and potential China shale gas and shale oil plays, Interpretation, 3 (2015) SJ1-SJ13.

[5] C.T. Montgomery, M.B. Smith, Hydraulic fracturing: History of an enduring technology, JPT, Journal of Petroleum Technology, 62 (2010) 26-32.

[6] R. Beckwith, Hydraulic fracturing: The fuss, the facts, the future, JPT, Journal of Petroleum Technology, 62 (2010) 34-41.

[7] Jackson, B. Robert, Vengosh, Avner, Davies, J. Richard, Carey, J. William, O'Sullivan, Francis, The Environmental Costs and Benefits of Fracking, Annual review of environment and resources, (2014).

[8] A. Kondash, A. Vengosh, Water Footprint of Hydraulic Fracturing, Environmental Science & Technology Letters, 2 (2015) 276-280.

[9] N.A. Ahmad, P.S. Goh, L.T. Yogarathinam, A.K. Zulhairun, A.F. Ismail, Current advances in membrane technologies for produced water desalination, Desalination, 493 (2020).

[10] B.C. Gordalla, U. Ewers, F.H. Frimmel, Hydraulic fracturing: a toxicological threat for groundwater and drinking-water?, Environmental Earth Sciences, 70 (2013) 3875-3893.

[11] W. Shang, A. Tiraferri, Q. He, N. Li, H. Chang, C. Liu, B. Liu, Reuse of shale gas flowback and produced water: Effects of coagulation and adsorption on ultrafiltration, reverse osmosis combined process, Sci. Total Environ., 689 (2019) 47-56.

[12] P. Tang, J. Li, T. Li, L. Tian, Y. Sun, W. Xie, Q. He, H. Chang, A. Tiraferri, B. Liu, Efficient integrated module of gravity driven membrane filtration, solar aeration and GAC adsorption for pretreatment of shale gas wastewater, J. Hazard. Mater., (2020).

[13] H. Chang, B. Liu, B. Yang, X. Yang, C. Guo, Q. He, S. Liang, S. Chen, P. Yang, An integrated coagulation-ultrafiltration-nanofiltration process for internal reuse of shale gas flowback and produced water, Sep. Purif. Technol., 211 (2019) 310-321.

[14] K.B. Gregory, R.D. Vidic, D.A. Dzombak, Water Management Challenges Associated with the Production of Shale Gas by Hydraulic Fracturing, Elements, 7 (2011) 181-186.

[15] T. Tong, K.H. Carlson, C.A. Robbins, Z. Zhang, X. Du, Membrane-based treatment of shale oil and gas wastewater: The current state of knowledge, Frontiers of Environmental Science and Engineering, 13 (2019).

[16] B. Wang, M. Xiong, P. Wang, B. Shi, Chemical characterization in hydraulic fracturing flowback and produced water (HF-FPW) of shale gas in Sichuan of China, Environmental Science and Pollution Research, 27 (2020) 26532-26542.

[17] F.X. Kong, Z.P. Wang, Z. Ji, J.F. Chen, C.M. Guo, G.D. Sun, Y.F. Xie, Organic fouling of membrane distillation for shale gas fracturing flowback water desalination: A special interest in the feed properties by pretreatment, Environmental Science: Water Research and Technology, 5 (2019) 1339-1348.

[18] D. Liu, J. Li, C. Zou, H. Cui, Y. Ni, J. Liu, W. Wu, L. Zhang, R. Coyte, A. Kondash, A. Vengosh, Recycling flowback water for hydraulic fracturing in Sichuan Basin, China: Implications for gas production, water footprint, and water quality of regenerated flowback water, Fuel, 272 (2020) 117621.
[19] A.W. Mohammad, Y.H. Teow, W.L. Ang, Y.T. Chung, D.L. Oatley-Radcliffe, N. Hilal, Nanofiltration membranes review: Recent advances and future prospects, Desalination, 356 (2015) 226-254.
[20] D. Zhou, L. Zhu, Y. Fu, M. Zhu, L. Xue, Development of lower cost seawater desalination processes using nanofiltration technologies — A review, Desalination, 376 (2015) 109-116.
[21] D. Rana, T. Matsuura, Surface Modifications for Antifouling Membranes, Chem. Rev., 110 (2010) 2448-2471.
[22] X. Zhao, R. Zhang, Y. Liu, M. He, Y. Su, C. Gao, Z. Jiang, Antifouling membrane surface construction: Chemistry plays a critical role, J. Membr. Sci., 551 (2018) 145-171.
[23] S. Jiang, Y. Li, B.P. Ladewig, A review of reverse osmosis membrane fouling and control strategies, Sci. Total Environ., 595 (2017) 567-583.
[24] T. Nguyen, F.A. Roddick, L. Fan, Biofouling of water treatment membranes: a review of the underlying causes, monitoring techniques and control measures, Membranes (Basel), 2 (2012) 804-840.
[25] E. Mohammad-Pajooh, D. Weichgrebe, G. Cuff, B.M. Tosarkani, K.-H. Rosenwinkel, On-site treatment of flowback and produced water from shale gas hydraulic fracturing: A review and economic evaluation, Chemosphere, 212 (2018) 898-914.
[26] W. Yu, T. Liu, J. Crawshaw, T. Liu, N. Graham, Ultrafiltration and nanofiltration membrane fouling by natural organic matter: Mechanisms and mitigation by pre-ozonation and pH, Water Res., 139 (2018) 353-362.
[27] F.-x. Kong, J.-f. Chen, H.-m. Wang, X.-n. Liu, X.-m. Wang, X. Wen, C.-m. Chen, Y.F. Xie, Application of coagulation-UF hybrid process for shale gas fracturing flowback water recycling: Performance and fouling analysis, J. Membr. Sci., 524 (2017) 460-469.
[28] Y. Liu, P. Tang, Y. Zhu, W. Xie, P. Yang, Z. Zhang, B. Liu, Green aerogel adsorbent for removal of organic compounds in shale gas wastewater: High-performance tuning and adsorption mechanism, Chem. Eng. J., 416 (2021) 129100.
[29] P. Tang, B. Liu, Y. Zhang, H. Chang, P. Zhou, M. Feng, V.K. Sharma, Sustainable reuse of shale gas wastewater by pre-ozonation with ultrafiltration-reverse osmosis, Chem. Eng. J., 392 (2020) 123743.
[30] P. Tang, W. Xie, A. Tiraferri, Y. Zhang, J. Zhu, J. Li, D. Lin, J.C. Crittenden, B. Liu, Organics removal from shale gas wastewater by pre-oxidation combined with biologically active filtration, Water Res., 196 (2021) 117041.
[31] Y.-C. Chiang, Y. Chang, C.-J. Chuang, R.-C. Ruaan, A facile zwitterionization in the interfacial modification of low bio-fouling nanofiltration membranes, J. Membr. Sci., 389 (2012) 76-82.
[32] T. Sun, Y. Liu, L. Shen, Y. Xu, R. Li, L. Huang, H. Lin, Magnetic field assisted arrangement of photocatalytic TiO2 particles on membrane surface to enhance membrane antifouling performance for water treatment, J. Colloid Interface Sci., 570 (2020) 273-285.
[33] M. He, K. Gao, L. Zhou, Z. Jiao, M. Wu, J. Cao, X. You, Z. Cai, Y. Su, Z. Jiang, Zwitterionic materials for antifouling membrane surface construction, Acta Biomater., 40 (2016) 142-152.
[34] Z. Wang, D. Hou, S. Lin, Composite Membrane with Underwater-Oleophobic Surface for Anti-Oil-Fouling Membrane Distillation, Environ. Sci. Technol., 50 (2016) 3866-3874.

[35] F.-x. Kong, G.-d. Sun, J.-f. Chen, J.-d. Han, C.-m. Guo, Z. Tong, X.-f. Lin, Y.F. Xie, Desalination and fouling of NF/low pressure RO membrane for shale gas fracturing flowback water treatment, Sep. Purif. Technol., 195 (2018) 216-223.
[36] X. Chen, T. Taguchi, Enhanced Skin Adhesive Property of Hydrophobically Modified Poly(vinyl alcohol) Films, ACS Omega, 5 (2020) 1519-1527.
[37] D.T. Auguste, R.K. Prud'homme, P.L. Ahl, P. Meers, J. Kohn, Polymer-Protected Liposomes: Association of Hydrophobically-Modified PEG with Liposomes, in: Polymeric Drug Delivery I, American Chemical Society, 2006, pp. 95-120.
[38] H. Huang, Y. Sun, L. Cui, Y. Ni, S. Li, W. Xing, W. Jing, Generation of Monodisperse Submicron Water-in-Diesel Emulsions via a Hydrophobic MXene-Modified Ceramic Membrane, Ind. Eng. Chem. Res., 59 (2020) 20349-20358.
[39] C. Zhao, X. Yu, X. Da, M. Qiu, X. Chen, Y. Fan, Fabrication of a charged PDA/PEI/Al2O3 composite nanofiltration membrane for desalination at high temperatures, Sep. Purif. Technol., 263 (2021) 118388.
[40] P. Kanagaraj, I.M.A. Mohamed, W. Huang, C. Liu, Membrane fouling mitigation for enhanced water flux and high separation of humic acid and copper ion using hydrophilic polyurethane modified cellulose acetate ultrafiltration membranes, Reactive and Functional Polymers, 150 (2020) 104538.
[41] H. Liu, Z. Ma, W. Yang, X. Pei, F. Zhou, Facile preparation of structured zwitterionic polymer substrate via sub-surface initiated atom transfer radical polymerization and its synergistic marine antifouling investigation, Eur. Polym. J., 112 (2019) 146-152.
[42] Q. Li, X. Zhang, H. Yu, H. Zhang, J. Wang, A facile surface modification strategy for improving the separation, antifouling and antimicrobial performances of the reverse osmosis membrane by hydrophilic and Schiff-base functionalizations, Colloids and Surfaces A: Physicochemical and Engineering Aspects, 587 (2020) 124326.
[43] C. Liu, A.F. Faria, J. Ma, M. Elimelech, Mitigation of Biofilm Development on Thin-Film Composite Membranes Functionalized with Zwitterionic Polymers and Silver Nanoparticles, Environ. Sci. Technol., 51 (2017) 182-191.
[44] M.S. Rahaman, H. Therien-Aubin, M. Ben-Sasson, C.K. Ober, M. Nielsen, M. Elimelech, Control of biofouling on reverse osmosis polyamide membranes modified with biocidal nanoparticles and antifouling polymer brushes, J Mater Chem B, 2 (2014) 1724-1732.
[45] D. Saeki, T. Tanimoto, H. Matsuyama, Anti-biofouling of polyamide reverse osmosis membranes using phosphorylcholine polymer grafted by surface-initiated atom transfer radical polymerization, Desalination, 350 (2014) 21-27.
[46] J. Wang, Z. Wang, J. Wang, S. Wang, Improving the water flux and bio-fouling resistance of reverse osmosis (RO) membrane through surface modification by zwitterionic polymer, J. Membr. Sci., 493 (2015) 188-199.
[47] G. Ye, J. Lee, F. Perreault, M. Elimelech, Controlled Architecture of Dual-Functional Block Copolymer Brushes on Thin-Film Composite Membranes for Integrated "Defending" and "Attacking" Strategies against Biofouling, ACS Appl. Mater. Interfaces, 7 (2015) 23069-23079.
[48] W.-W. Yue, H.-J. Li, T. Xiang, H. Qin, S.-D. Sun, C.-S. Zhao, Grafting of zwitterion from polysulfone membrane via surface-initiated ATRP with enhanced antifouling property and biocompatibility, J. Membr. Sci., 446 (2013) 79-91.
[49] H. Chang, T. Li, B. Liu, C. Chen, Q. He, J.C. Crittenden, Smart ultrafiltration membrane fouling control as desalination pretreatment of shale gas fracturing wastewater: The effects of backwash water, Environ. Int., 130 (2019) 104869.
[50] K. Matyjaszewski, Atom Transfer Radical Polymerization (ATRP): Current status and future perspectives, Macromolecules, 45 (2012) 4015-4039.

[51] K. Matyjaszewski, D. Hongchen, W. Jakubowski, J. Pietrasik, A. Kusumo, Grafting from surfaces for "everyone": ARGET ATRP in the presence of air, Langmuir, 23 (2007) 4528-4531.
[52] W. Xie, A. Tiraferri, X. Ji, C. Chen, Y. Bai, J.C. Crittenden, B. Liu, Green and sustainable method of manufacturing anti-fouling zwitterionic polymers-modified poly(vinyl chloride) ultrafiltration membranes, J. Colloid Interface Sci., 591 (2021) 343-351.
[53] M. He, T. Li, M. Hu, C. Chen, B. Liu, J. Crittenden, L.-Y. Chu, H.Y. Ng, Performance improvement for thin-film composite nanofiltration membranes prepared on PSf/PSf-g-PEG blended substrates, Sep. Purif. Technol., 230 (2020) 115855.
[54] S. Hong, M. Elimelech, Chemical and physical aspects of natural organic matter (NOM) fouling of nanofiltration membranes, J. Membr. Sci., 132 (1997) 159-181.
[55] W. Wu, R.F. Giese, C.J. van Oss, Stability versus flocculation of particle suspensions in water—correlation with the extended DLVO approach for aqueous systems, compared with classical DLVO theory, Colloids and Surfaces B: Biointerfaces, 14 (1999) 47-55.
[56] A. Tiraferri, Y. Kang, E.P. Giannelis, M. Elimelech, Highly Hydrophilic Thin-Film Composite Forward Osmosis Membranes Functionalized with Surface-Tailored Nanoparticles, ACS Appl. Mater. Interfaces, 4 (2012) 5044-5053.
[57] C.Y. Tang, Y.-N. Kwon, J.O. Leckie, Effect of membrane chemistry and coating layer on physiochemical properties of thin film composite polyamide RO and NF membranes: II. Membrane physiochemical properties and their dependence on polyamide and coating layers, Desalination, 242 (2009) 168-182.
[58] A. Simon, W.E. Price, L.D. Nghiem, Influence of formulated chemical cleaning reagents on the surface properties and separation efficiency of nanofiltrationmembranes, J. Membr. Sci., 432 (2013) 73-82.
[59] M.F. Jimenez Solomon, Y. Bhole, A.G. Livingston, High flux membranes for organic solvent nanofiltration (OSN)—Interfacial polymerization with solvent activation, J. Membr. Sci., 423-424 (2012) 371-382.
[60] Y. Li, E. Wong, Z. Mai, B. Van der Bruggen, Fabrication of composite polyamide/Kevlar aramid nanofiber nanofiltration membranes with high permselectivity in water desalination, J. Membr. Sci., 592 (2019).
[61] M.R. De Guzman, C.K.A. Andra, M.B.M.Y. Ang, G.V.C. Dizon, A.R. Caparanga, S.-H. Huang, K.-R. Lee, Increased performance and antifouling of mixed-matrix membranes of cellulose acetate with hydrophilic nanoparticles of polydopamine-sulfobetaine methacrylate for oil-water separation, J. Membr. Sci., 620 (2021) 118881.
[62] Q. Shi, Y. Su, W. Zhao, C. Li, Y. Hu, Z. Jiang, S. Zhu, Zwitterionic Polyethersulfone Ultrafiltration Membrane with Superior Antifouling Property, J. Membr. Sci., 319 (2008) 271.
[63] Z. He, D.J. Miller, S. Kasemset, D.R. Paul, B.D. Freeman, The effect of permeate flux on membrane fouling during microfiltration of oily water, J. Membr. Sci., 525 (2017) 25-34.
[64] J. Guo, X. Zhu, Q. Wang, W. Liu, Y. Wang, The combination effect of preozonation and CNTs layer modification on low-pressure membrane fouling control in treating NOM and EfOM, J. Membr. Sci., 627 (2021) 119225.
[65] M. Zhang, X. Zhou, L. Shen, X. Cai, F. Wang, J. Chen, H. Lin, R. Li, X. Wu, B.-Q. Liao, Quantitative evaluation of the interfacial interactions between a randomly rough sludge floc and membrane surface in a membrane bioreactor based on fractal geometry, Bioresour. Technol., 234 (2017) 198-207.
[66] C. Liu, D. Song, W. Zhang, Q. He, X. Huangfu, S. Sun, Z. Sun, W. Cheng, J. Ma, Constructing zwitterionic polymer brush layer to enhance gravity-driven membrane performance by governing biofilm formation, Water Res., 168 (2020) 115181.

602 [67] N. Subhi, A.R.D. Verliefde, V. Chen, P. Le-Clech, Assessment of physicochemical
603 interactions in hollow fibre ultrafiltration membrane by contact angle analysis, J. Membr.
604 Sci., 403-404 (2012) 32-40.

605 **Graphical abstract**

606